Physics of the Earth and Planetary Interiors 175 (2009) 26–36

Contents lists available at ScienceDirect

Physics of the Earth and Planetary Interiors

journal homepage: www.elsevier.com/locate/pepi

Source study and tectonic implications of the historic 1958 Las Melosas crustal earthquake, Chile, compared to earthquake damage

Patricia Alvarado[a,b,*], Sergio Barrientos[c], Mauro Saez[b], Maximiliano Astroza[d], Susan Beck[e]

[a] CONICET, Universidad Nacional de San Juan, Meglioli 1160 S, 5400 Rivadavia, San Juan, Argentina
[b] Departamento de Geofísica y Astronomía, Universidad Nacional de San Juan, Meglioli 1160 S, 5400 Rivadavia, San Juan, Argentina
[c] Servicio Sismológico Nacional, Departamento de Geofísica, Universidad de Chile, Blanco Encalada 2002 Santiago, Chile
[d] Departamento de Ingeniería Civil, Universidad de Chile, Blanco Encalada 2002 Santiago, Chile
[e] Department of Geosciences, University of Arizona, Gould Simpson Bldg. #77 1040 E Four Street, Tucson, AZ 85721, USA

ARTICLE INFO

Article history:
Received 17 April 2007
Accepted 3 March 2008

Keywords:
Crustal seismicity
Andean Cordillera
Neotectonics
Seismic hazard

ABSTRACT

The 4 September 1958 earthquake has been the largest event recorded at shallow depths in the western flank of the Andes on Chilean territory. New estimates of fault orientation, depth and size have been carried out using modern techniques of body-wave modeling. Two possible fault planes solutions with right-lateral displacement on an east-west fault or left-lateral displacement on a north-south fault nucleated at 5–9 km depth produce the best fit to teleseismic recordings. A seismic moment M_0 of 0.227×10^{19} N m associated with a moment-magnitude M_w of 6.3 has been estimated with these techniques, which is a more reliable estimation of earthquake size than the 0.4–0.7 units larger surface-wave magnitude M_s earlier reported. Although no surface rupture for the 1958 Las Melosas crustal earthquake was reported, the displacement along east-west structures like that one suggested for one of the fault plane in our focal mechanism solution seems to be an efficient mechanism to accommodate differences in shortening from north to south in the High Andean Cordillera. Reports on damage, landslide effects as well as re-analysis of intensities associated with the new seismic source estimations for the 1958 Las Melosas earthquake are presented to further estimate the hazard to which this zone, and others along the western foothills of the Andes, is exposed.

1. Introduction

The High Andean Cordillera is the main result of the subduction of the Nazca plate beneath the South American plate (Fig. 1). This active margin between 30°S and 35°S is characterized by a convergence rate of about 6.7 cm/yr along an azimuth of about 78° (Vigny et al., in this issue). This convergence generates three main seismogenic zones: along the coast there are large shallow (0–50 km) interplate thrust earthquakes, large deeper (70–100 km) tensional as well as compressional events within the subducting Nazca plate, and very shallow seismicity (0–35 km) within the overriding South American plate. Deeper seismicity (100–650 km) occurs further north of this region, beneath Bolivia and north-western Argentina (Barazangi and Isacks, 1976; Cahill and Isacks, 1992; Anderson et al., 2007).

The large ($M > 8$) interplate thrust earthquakes – usually accompanied by noticeable coastal elevation changes and, depending on the amount of seafloor vertical displacement, by catastrophic tsunamis – are located along the coast from Arica (18°S, the northernmost extreme of coastal Chile) to the triple junction at Taitao Peninsula (46°S). Their rupture zones are limited to the coupled region between the Nazca and South American plates which extends usually down to 45–53 km depth (Tichelaar and Ruff, 1991) and their lengths can reach well over one thousand kilometers long. Return periods for magnitude ~8 events are of the order of 80–130 years for any given region in Chile, but about a dozen years when the subduction plate boundary along the coast of Chile is considered as a whole. Thus, megathrust earthquakes seem to have much longer return periods, of the order of a few centuries for any given region (Cifuentes, 1989; Barrientos and Ward, 1990; Cisternas et al., 2005), while no estimates exist for shallow (depth < 35 km) continental seismicity recurrence.

The most damaging earthquake in terms of losses of human lives in Chilean history is the 1939 Chillán event. This earthquake, which produced more than 28,000 fatalities, is the reminder of the destructive capabilities of these Nazca intraplate intermediate-depth events (Beck et al., 1998). Other examples of these type of events in Chile are the Calama 1950 (Kausel and Campos, 1992), the Punitaqui 1997 (Pardo et al., 2002) and the Tarapacá 2005 (Peyrat et al., 2006) earthquakes. Large stress drops at these ~100-km depth

* Corresponding author at: Departamento de Geofísica y Astronomía, Universidad Nacional de San Juan, Meglioli 1160 S (5400) Rivadavia, San Juan, Argentina.
Tel.: +54 264 423 4129x177; fax: +54 264 423 4980.
E-mail address: alvarado@unsj.edu.ar (P. Alvarado).

0031-9201/$ – see front matter © 2009 Elsevier B.V. All rights reserved.
doi:10.1016/j.pepi.2008.03.015

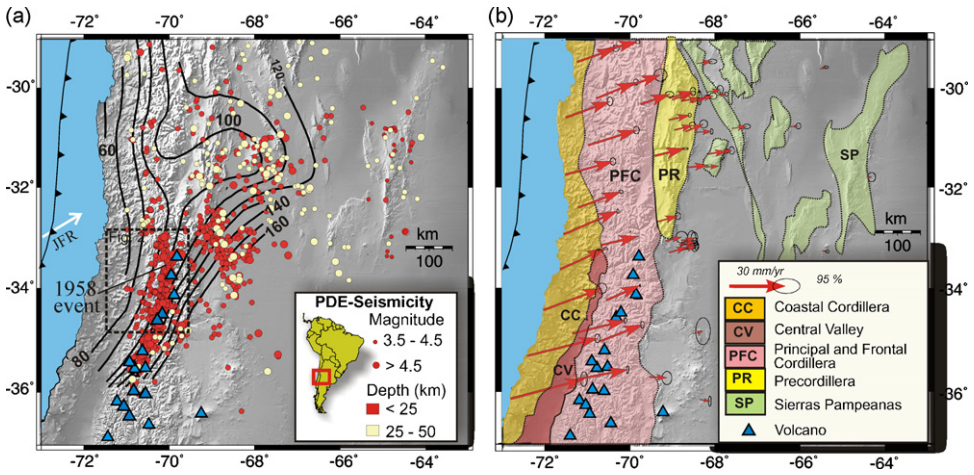

Fig. 1. Regional tectonic maps of the area of study. (a) Intraplate crustal seismicity of the South American plate reported by the Chile and Argentina seismic network catalogues during the last 20 years. Contours in km of the approximate top of the subducted Nazca plate from Anderson et al. (2007). White arrow represents the approximate location of the subducting Juan Fernández Ridge and blue triangles, the modern volcanic arc. Location of Fig. 2 including the 1958 Las Melosas, Chile earthquake epicenter is shown by a dashed-line rectangle. (b) Major tectonic provinces from Ramos et al. (2002) and GPS velocity vectors with their uncertainty-ellipses from Brooks et al. (2003).

sources have been proposed as the component that produces the large destruction (Kausel, 1991).

The shallow sesmicity is placed along the continental crust of the High (Principal and Frontal) Andean Cordillera and its backarc region, capable of generating moderate to large-sized damaging earthquakes (Barrientos, 2007; INPRES, 2009). These crustal events are still observed in the Argentinean Sierras Pampeanas uplifts as far as 600–800 km east from the trench, in good correlation with a northeast elongated flat subduction of the Nazca plate at about 100-km depth and ~31°S (Fig. 1) (Gustcher et al., 2000; Anderson et al., 2007). The abundant Andean backarc seismicity extends into the High Cordillera south of 33°S overriding a segment of steeper (normal) subduction with typical active volcanism (Kay et al., 1991; Barrientos et al., 2004; Anderson et al., 2007). Two earthquakes that occurred in the western flank of the High Cordillera in August and September of 1958 had shallow (20 km) depths roughly above the change in dip angle of the subduction, from a subhorizontal mode to a steep angle mode (Fig. 1). Studies of the seismic sources for these events and other larger crustal seismic events in this southern segment indicate shallow depths and mainly strike-slip focal mechanism solutions, although the 1958 earthquake solutions exhibit an opposite direction of slip ("rake" angle) (Lomnitz, 1960; Piderit, 1961; Pardo and Acevedo, 1984).

Recent studies by Barrientos et al. (2004), Leyton et al. (in this issue) and Sepúlveda et al. (2008) point out the threat from these shallow-depth earthquakes and their effects in the Chilean Cordillera and its western flank posed to populated centers in Chile, perhaps underestimated in existing seismic hazard estimations. Given the tectonic and seismic hazard implications of this type of seismicity, we present a quantitative seismic analysis of the historical crustal earthquake on 4 September 1958 that caused damage in Las Melosas, central Chile (Fig. 1a) (Lomnitz, 1960; Piderit, 1961). Our study is based on waveform modeling of paper seismograms recorded at teleseismic distances and compiled historic information.

2. Seismotectonic setting

Major tectonic provinces with a north-south orientation in South America between 30°S and 35°S correlate with variations in the angle of subduction of the Nazca plate (Fig. 1) (Barazangi and Isacks, 1976; Jordan et al., 1983). These units mainly reflect the eastward shift of the magmatic arc through time with the consequent upper plate deformation (Ramos et al., 2002). From west to east they comprise the *Coastal Cordillera* with Paleozoic metamorphic and Mesozoic basic magmatic rocks (Parada et al., 1991); the *Central Valley* with Neogene and Quaternary sediments overlying Mesozoic basement (Charrier et al., 2007); the *Principal Cordillera* with Oligocene to Miocene volcanic and sedimentary rocks including the current active arc south of ~33°S (Stern, 2004); the Precambrian-Paleozoic basement outcrops of the *Frontal Cordillera* with thin and thick-skinned deformation (Cristallini and Ramos, 2000; Giambiagi et al., 2003); the *Precordillera* characterized by the thin-skinned fold and thrust belt made up of Cambrian-Ordovician carbonate platform rocks and Silurian, Devonian foreland deposits and Late Paleozoic continental and marine sediments (Baldis and Bordonaro, 1981; Ramos, 1999); and the basement-cored *Sierras Pampeanas* uplifted by thick-skinned deformation, and discontinued by intervening valleys (Jordan and Allmendinger, 1986). The tectonic evolution of the entire region includes periods of contractional and extensional episodes since Paleozoic, which have controlled folding and faulting with reactivation and inversion of pre-existing structures at local and regional scales (Charrier et al., 2002; Ramos et al., 2002).

Crustal seismic activity in the South American plate also correlates with variations in the geometry of the subducted Nazca plate and differences in crustal Andean structures (Fig. 1) (Alvarado et al., 2007). Frequent and damaging large crustal earthquakes have occurred in the Andean backarc of Argentina in 1861, 1894, 1944, 1977 and 1985 (Kadinsky-Cade, 1985; Zamarbide and Castano, 1993; Langer and Hartzell, 1996; Mingorance, 2006; Alvarado and Beck, 2006; INPRES, 2009). Their hypocenters were located between 10 km and 30 km depths within the upper levels of a mafic and thicker (~55-km) continental crust, which overrides a nearly horizontal subducted Nazca plate and its transition to "normal" (~30° dip to the southeast). This correlates with the inland projection of the subducting Juan Fernández oceanic ridge (Fig. 1a) (Yañez et al., 2001; Anderson et al., 2007; Alvarado et al., 2009). This high seismic activity shifts to the High Cordillera south of ~33°S generating earthquakes in the upper 20 km of the Andean crust and its western flank (Fig. 1) (Alvarado, 1998; Barrientos et al., 2004). In this region the slab subducts (~30° to the east) normally and the Andean ~45-km thick crust exhibits partial melting with intermediate-to-mafic composition (Kay et al., 1991; Alvarado et al., 2007). Several historic and modern crustal earthquakes were recorded by global seismic networks like the 1958, 1987, 2001 and 2004 events (Barrientos and Eisenberg, 1988; Charrier et al., 2004; Alvarado et al., 2005). With the only exception of the 1958 earth-

quake, seismic source determinations based on waveform modeling for these larger crustal seismic events in the High Cordillera indicate focal mechanisms with right-lateral strike-slip along fault-plane solutions of north-south trending or the alternative left-lateral displacement along east-west trending fault plane solutions (Fig. 2) (Alvarado et al., 2009; Harvard-Centroid Moment Tensor catalogue, 2009). A discordant style of deformation based on first-motion data has been suggested for the composite focal mechanism of the 1958 Las Melosas earthquake (left-lateral strike-slip type on a steep north-south trending fault-plane solution or right-lateral strike-slip along an east-west oriented fault-plane solution) (Fig. 2) (Lomnitz, 1960; Piderit, 1961; Pardo and Acevedo, 1984).

Current deformation of the upper South American plate is also evidenced by GPS surveys (Brooks et al., 2003; Klotz et al., 2006; Hoffmann-Rothe et al., 2006; Vigny et al., in this issue). An important decay of the GPS velocity vectors, with respect to fixed stations in cratonic South America, occurs from the coast to the east, which is more pronounced to the south of 33°S. Although very scarce data, GPS velocity vectors from Brooks et al. (2003) show a slight clockwise rotation from the coast to the Andean backarc in this southern segment, which also show larger uncertainties (Fig. 1b). Results from geologic investigations suggest there is a different style and magnitude of deformation at Cenozoic times around ~33°S with a southward decrease in shortening in the Principal Cordillera that involve significant thin-skinned deformation in the north and mainly thick-skinned deformation in the south (Ramos et al., 1996; Giambiagi and Ramos, 2002; Vietor and Echtler, 2006). Such estimations are based on balanced cross-sections, which consider the same initial crustal thickness (Allmendinger et al., 1990; Cristallini and Ramos, 2000). Studies of global climate change, sediment flux to the trench and tectonic uplift in Late Cenozoic indicate the Juan Fernández Ridge intersection at around 33°S might play an important role in the mountain building process by changing the mechanical properties of the plate boundary and by shallowing the subduction angle which led to upper-plate weakening (north of 33°S) and inhibiting upper-plate shortening (south of 33°S) of the continental South American plate (Vietor and Echtler, 2006).

3. The 1958 Las Melosas, Chile earthquake

The 4 September 1958 earthquake is the largest seismic event in the last century located in the transition zone between the seismically active Andean backarc north of 33°S and the active High Cordillera crust, south of this latitude. Although somewhat uncertain, relocation studies report an epicenter at 33.826°S and 70.140°W and a focal depth of 35 km (Engdahl et al., 1998). According to the United States Coast and Geodetic Survey-USCGS (BSSA, 1959) this crustal earthquake occurred on a Sunday evening at 21 h, 51 min and 08 s (Universal Time) and had an approximate magnitude 6.7–7 based on estimations of surface waves from station PAS (Pasadena, USA) or 6.7 from station BER (Berkeley, USA).

Local reports indicate four deaths nearby Las Melosas, hundreds of injured people and major damage in Las Melosas, Chile about 60 km southeast from Santiago, the main populated center by that time (BSSA, 1959; Piderit, 1961; El Correo de Santiago, 2009). Studies of the effects of this earthquake indicate maximum Modified Mercalli (MM) seismic intensity IX–X in Las Melosas and El Volcán (Flores et al., 1960). Santiago recorded maximum MM seismic intensities slightly less than VI (Lomnitz, 1960) (Fig. 2).

Although global seismic catalogues include only one earthquake on 4 September 1958, Lomnitz (1960) and Piderit (1961) have reported the occurrence of more than one seismic event (at least three) separated by a few minutes and of similar sized-magnitudes. In fact, these authors assigned a 6.9 magnitude for the three subevents, but Flores et al. (1960) reported 6.9, 6.7 and 6.8, respectively. We note these estimations of the seismic magnitudes are mainly based on historical intensity reports (Lomnitz, 1970a).

According to reports from Sewell, ~55 km south of Santiago (Fig. 2b), at least seven earthquakes a day were recorded 6 weeks prior to the mainshock (BSSA, 1959; Lomnitz, 1970a). Of this foreshock sequence, only one seismic event has been reported by the USCGS on 28 August 1958 at 9 h, 36 min and 06 s (Universal Time) which caused damage in Las Melosas (BSSA, 1959; Saint-Amand and Ericksen, 1964; El Correo de Santiago, 2009). Because of this previous seismic activity, people in the epicentral area of the 4 September 1958 mainshock were evacuated. The 28 August event, in fact, pro-

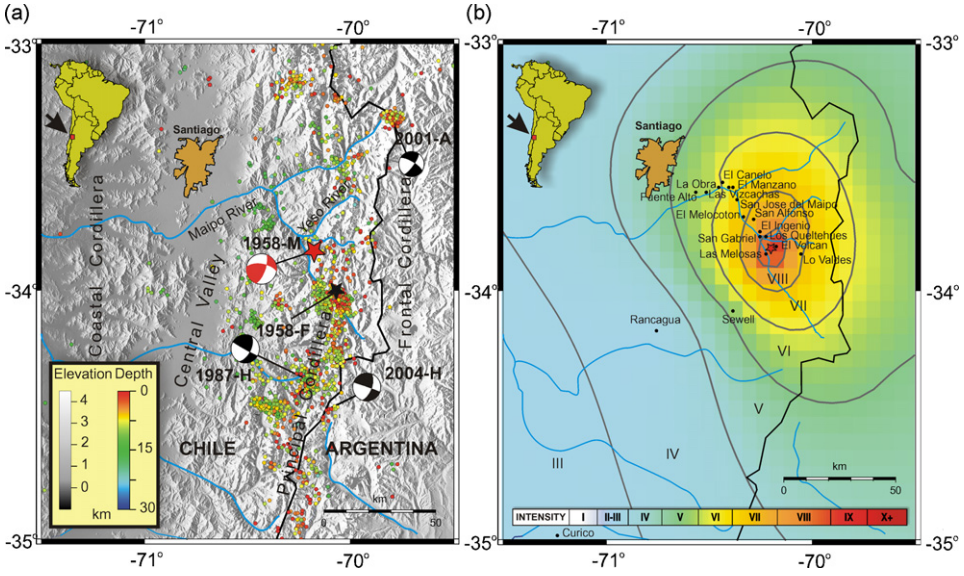

Fig. 2. (a) Relocated seismicity between 1995 and 2005 from Barrientos et al. (2004). Focal mechanisms are lower-hemisphere projections with compressional dark-quadrants for the 4 September 1958 earthquake (1958-M, this study) and other seismogram modeling solutions from Alvarado et al., 2005 (2001-A) and Harvard CMT catalogue (1987-H and 2004-H). Tectonic provinces and location of the larger foreshock (1958-F) on 28 August 1958 are also shown. (b) Map of the MSK seismic intensities listed in Table 2 recalculated by Sepúlveda et al. (2008) for the Las Melosas crustal earthquake on 4 September 1958. We also show our interpolation of the MSK intensities by grey contours. Note the maximum MSK intensity IX encircles the localities of Las Melosas and El Volcán for the 4 September earthquake.

duced large damage to the water channels that serve the El Volcán and Los Queltehues hydroelectric power plants (DIC, 1958). Recent studies by Astroza and Sepúlveda (2006) have confirmed this observation, which correlates with the occurrence of the 28 August 1958 earthquake located at 33.5°S and 69.5°W (BSSA, 1959) or relocated at 34.01°S; 70.06°W by the ISS close to the earthquake event on 4 September 1958 (Fig. 2a). Pardo and Acevedo (1984) list a focal depth of 15 km and magnitude M_s of 6.0 for the 28 August 1958 event.

The seismic events in August and September of 1958 took place in the upper Maipo River (Fig. 2), a region adjacent to north-south trending, west vergent reverse faults in the foothills of the High Cordillera (Thiele, 1980). At least two landslides, which are still preserved, were triggered by the 1958 earthquakes (Casas et al., 2005). Both landslides are likely related to the events on 28 August and 4 September, respectively (see Sepúlveda et al., 2008 for a complete analysis). On 6 December 1850 at 6 h, 42 min (Universal Time) a magnitude 7–7.5 earthquake, similar to the earthquake on 4 September 1958, hit the Maipo Valley killing two persons and causing widespread damage. The MM seismic intensity in Santiago was about VII. Large rockslides were reported 14 km south of San José indicating a similar epicenter to the 4 September 1958 event (Lomnitz, 1970b).

Composite focal mechanism solutions using P-wave first motions for the three events on 4 September 1958 indicate solutions of approximate strike N13°E, dip 78° to the west and left lateral motion or strike N74°W, dip 82° to the north and right lateral motion as the possible activated fault planes (Lomnitz, 1960; Piderit, 1961; Pardo and Acevedo, 1984). Focal depths are consistently shallow (~10 km). The solution for the event on 28 August 1958 is similar with fault planes of north-south strike, dip 75° to the west and left lateral motion and strike N84°W, dip 70° to the north and right lateral motion (Pardo and Acevedo, 1984). Unfortunately, there is no obvious evidence of surface rupture associated with the seismic events in 1958 (Pardo and Acevedo, 1984; Lavenu and Cembrano, 1999) to help discriminate between the two possible active fault planes.

In this study we present seismic modeling of teleseismic P-waves to determine the focal mechanism, focal depth, seismic moment, magnitude and source time function for the first event in the sequence of earthquakes of 4 September 1958. In addition, we compare these seismic source results with the corresponding seismic intensities recently recalculated by Sepúlveda et al. (2008).

4. Damage and seismic intensities

The 1958 Las Melosas earthquake provides the only documented example in the region of the effects of strong shaking related with a shallow crustal earthquake in a subduction environment where high magnitude interplate and in less extent, intermediate-depth intraplate earthquakes, are far more common. Shaking intensity data for the earthquakes are crucial for estimating earthquake hazards of future Chilean crustal earthquakes since similar events will no-doubt recur.

The earthquake damage was concentrated in mining and industrial facilities (electrical generation and water supply plants) (Figs. 2 and 3), and in one and two-story houses (Figs. 4 and 5). Many of these buildings did not have an earthquake-resistant design and were built with materials available from the immediate area. Thus the stock of single buildings can be classified as unreinforced stone or rubble masonry, adobe houses, diagonally braced wooden frame infilled with adobe or concrete and partially or totally confined stone masonry. With the exception of the latter (Fig. 6), the others suffered heavy damage like large and deep cracks in walls.

In view of the importance of the 1958 earthquake, Sepúlveda et al. (2008) have revised the seismic intensities assigned by Flores et al. (1960) and Lomnitz (1960) and estimated new intensity values over VI in the area damaged by this earthquake. The new intensity results are mainly based on analysis of historical documents (Rosenberg, 1958; Flores et al., 1960; Piderit, 1961) and direct field observations (Sepúlveda et al., 2008). Thus these intensity values consider the distribution of damage in the different types of structures, which are classified according to their vulnerability

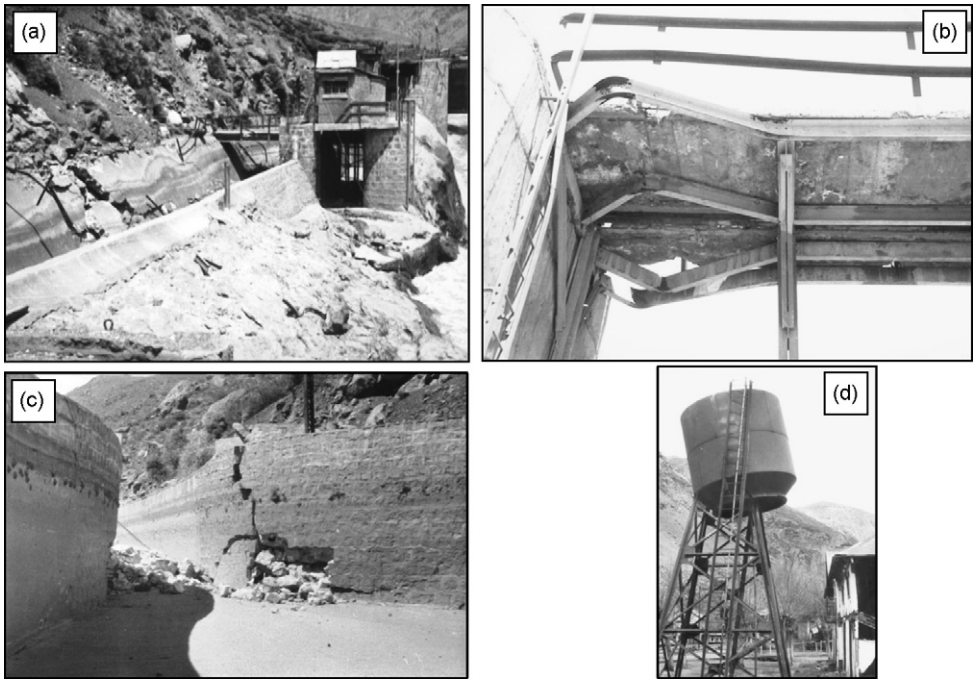

Fig. 3. Damage in industrial structures and facilities after the event on 4 September 1958 (DIC, 1958); see location in Fig. 2. (a) Damage in Channel Maipo, sector Intake near Las Melosas. (b) Damage in footbridge of Channel Maipo Intake near Las Melosas. (c) Damage in surge chamber of Channel El Volcán, near Los Queltehues. (d) Damage in elevated water (steel) tank located at El Volcán railstation.

Fig. 4. Damage in unreinforced masonry house in El Volcán (a) and Las Melosas (b) (DIC, 1958) after the event on 4 September 1958; see location in Fig. 2.

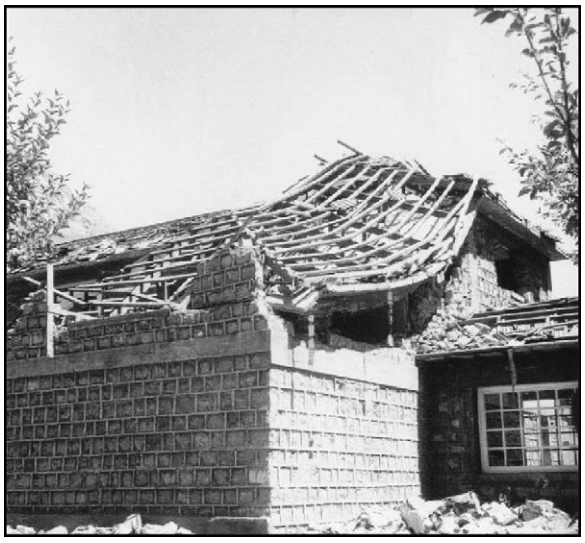

Fig. 5. Damage in two story unreinforced stone masonry buildings in Las Melosas after the earthquake on 4 September 1958 (DIC, 1958); see location in Fig. 2.

Table 1
Definition of vulnerability classes (modified from Sepúlveda et al., 2008).

Vulnerability class	Type of structure
A	Stone masonry and adobe houses
B	Stone masonry fixed with cement mortar. Unreinforced masonry houses. Braced wooden frame infilled with adobe
C	Reinforced and confined masonry houses

(Table 1) using the MSK (Medvedev, Sponheuer, Karnik) intensity scale. The MSK scale relates damage distribution with vulnerability class (Karnik et al., 1984; Monge and Astroza, 1989).

Because of the scarce population in the epicentral area of the 1958 earthquake at that time, the intensity values were only determined in 15 small towns located at distances of less than ~80 km from the earthquake epicenter. Sepúlveda et al. (2008) show how the photographs (DIC, 1958) and damage reports were used to assign MSK intensities at specific places. We interpolated the MKS intensity data for the 1958 earthquake. Table 2 and Fig. 2b compile these intensities, which show peak values of VIII–IX in the epicentral area with a quick attenuation pattern, being reduced from IX to VI over a distance of just 40 km. The intensities in the earthquake-felt area $I_{MSK} \leq V$, were obtained from the newspaper "El Mercurio" (1958). In this region, damage to buildings and other earthquake effects like rockfalls and landslides completely disappeared. Astroza and Sepúlveda (2006) used evidences of rocksfalls to delimitate the intensity VI based on comparison with other earthquakes in Chile. In Santiago, documented reports state there was no damage to buildings although the shock was very appreciable; thus an intensity V was assigned (Table 2 and Fig. 2b).

5. Teleseismic data and methods

Seismic waveforms for historical earthquakes prior to the World Wide Standard Seismograph Network (WWSSN) operation are difficult to obtain. If existing, the historic seismograms are on smoked paper or common ink recordings on standard paper archived in a few seismic observatories around the world. We have collected vertical-component paper seismograms and instrument responses from five seismic observatories for the 1958 earthquake (Fig. 7b and Table 3). We have scanned and digitized all available analog seismograms using the interactive software SeisDig (Bromirski and

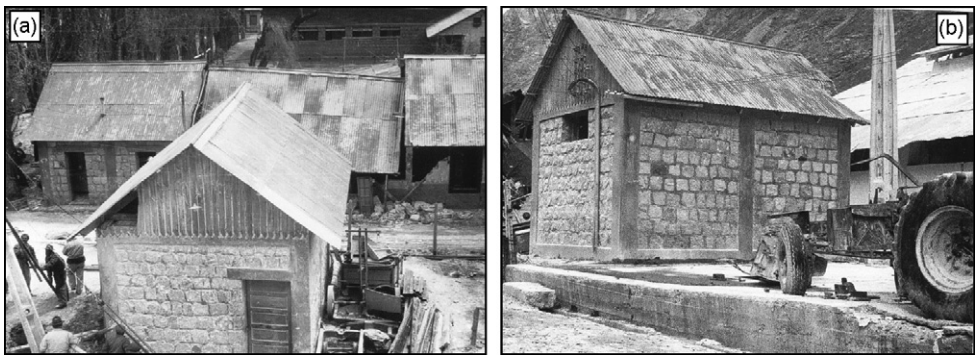

Fig. 6. Confined stone masonry buildings without damage in El Volcán after the earthquake on 4 September 1958 (DIC, 1958).

Table 2
Intensities from Sepúlveda et al. (2008) for the 1958 earthquake.

Locality	Latitude	Longitude	MSK seismic intensity
Puente Alto	−33°36′	−70°34′	V–VI
Las Vizcachas	−33°36′	−70°31′	V–VI
La Obra	−33°35′	−70°27′	V–VI
El Canelo	−33°34′	−70°26′	VI
El Manzano	−33°35′	−70°24′	VI
Guayacán	−33°35′	−70°23′	VI–VII
San José de Maipo	−33°38′	−70°22′	VI–VII
El Melocotón	−33°42′	−70°20′	VII
San Alfonso	−33°43′	−70°17′	VII
El Ingenio	−33°46′	−70°15′	VII–VIII
San Gabriel	−33°47′	−70°15′	VII–VIII
Los Queltehues	−33°47′	−70°13′	VIII
Las Melosas	−33°51′	−70°13′	VIII–IX
El Volcán	−33°49′	−70°10′	IX
Lo Valdés	−33°51′	−70°03′	≤VII
Santiago	−33°27′	−70°38′	V
Valparaíso[a]	−33°02′	−71°38′	III
San Felipe[a]	−32°45′	−70°43′	III
La Calera[a]	−32°45′	−71°12′	III
Sewel[a]	−34°05′	−70°23′	IV
Rancagua[a]	−34°10′	−70°45′	III
Curicó[a]	−34°59′	−71°14′	III
Curepto[a]	−35°05′	−72°01′	III
Talca[a]	−35°25′	−71°35′	III
Cauquenes[a]	−35°58′	−72°19′	II

[a] El Mercurio newspaper, 1958.

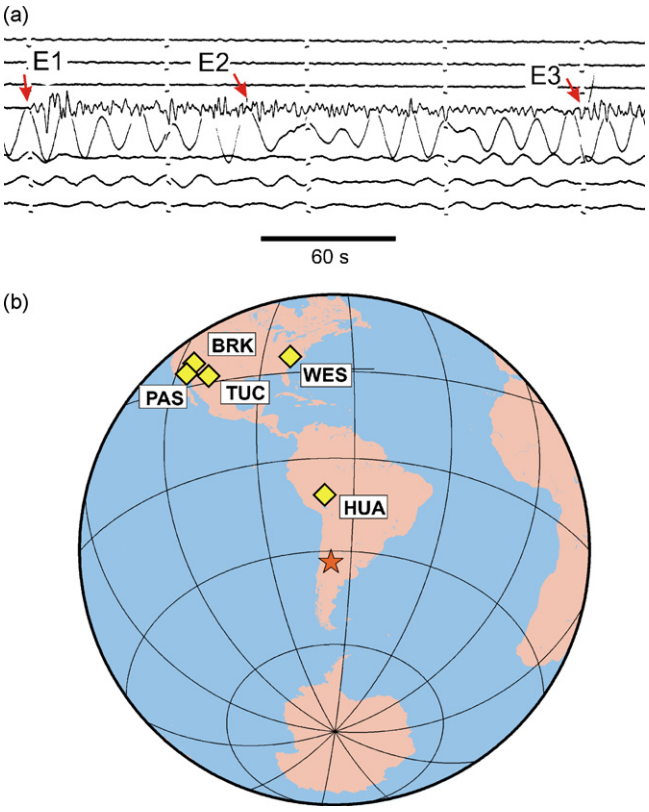

Fig. 7. (a) Example of a vertical component seismogram recorded at 76° epicentral distance and 146° backazimuth by station TUC (Tucson, USA) for the 4 September 1958 earthquake. Three different seismic events (E1, E2 and E3) are observed in a time window of 4–5 min. For these data, Event E1 is the only seismic event with a clear arrival. (b) Distribution of seismic stations used in this study with respect to the 1958 earthquake location (see Table 1 for details).

Chuang, 2003) (Fig. 7a). We also used Sac2000 (Goldstein et al., 1999) for data preparation.

We did a grid search to estimate the focal mechanism using polarities of the P-wave first-motion data in Table 3 (Fig. 7b). Data from the vertical-component record at station Huancayo in Perú only provided polarity information (Table 3). Because of the limited data availability for this historical earthquake, we also utilized vertical-component seismograms to model teleseismic P-waves recorded at epicentral distances between 76° and 86°. We used a waveform modeling technique that determines the source time function from an inversion of multi-station data considering a minimization of the scatter in the waveform amplitudes (Ruff, 1989). Instrument responses were convolved with synthetic seismic displacements before comparison with observed data. Better matches between observed and synthetic seismograms occur for better-predicted amplitude phases and their respective timing. We assumed the focal mechanism parameters (strike, dip and rake) and the focal depth. The source earth model consisted of a P-wave velocity of 6.2 km/s and an average density of 2.7 g/cm^3. We used a 2-s interval for the source time function and 40-s length of the teleseismic P-wave records.

In order to improve our estimate of uncertainties on seismic source parameters, we have performed a full grid search around the focal mechanism parameters and focal depth. Thus we computed several inversions for a set of fixed strike, dip, rake and focal-depth values using the described method by Ruff (1989). For each inversion, we obtained the source time function, the amplitude misfit-errors between observed and synthetic waveforms and the corresponding synthetic seismograms (Figs. 8 and 9).

6. Results and discussion

We have identified at least three events in the sequence of earthquakes on 4 September 1958 as found previously by other authors (Lomnitz, 1960; Piderit, 961). Fig. 7a shows a vertical-component seismogram from station TUC (Tucson, USA). This record clearly shows the first event E1, and possible events E2 and E3 approximate arrivals at 1.5 min and 4 min after the first event E1, respectively. We were able to identify a similar sequence of seismic events on the record from station PAS (Pasadena, USA) (Fig. 7b). Accurate arrival reading and modeling of the waveforms for these events (E2 and E3), however, is difficult because of their interference with the seismic coda from the first event. Thus we only modeled the first event E1 as shown in Fig. 8.Our best results for the first event on 4 September 1958 indicate a seismic moment M_0 of 0.227 × 10^{19} N m and a duration of 8–10 s for the source time function. Consider-

Table 3
Seismic data used in the source study of the 1958 earthquake.

Station	Comp.	Lat.	Long.	H (m)	Delta	Az	Baz	Type of Inst.	To	Tg	Damp	V_m	Speed	Take-off
WES	Z	42.38	−71.32	60	75.8	359.1	179	Benioff	1	60	0.7	3000	30 mm/min	19
BRK	Z	37.87	−112.26	49	86.2	321.3	138.8	Galitzin	12	12	0.6	600	30 mm/min	16
TUC	Z	32.25	−110.83	770	76	325.3	146	Benioff	1	77	0.8	3000	30 mm/min	18
PAS	Z	34.14	−118.17	295	81.2	321.4	141.2	Benioff	1	90	0.8	3000	30 mm/min	17

Comp. is the seismic component (Z, vertical component); Lat., the station location latitude; Long., the station location longitude; H, the station altitude; Δ, the epicentral distance; Az, the azimuth to the station; Baz, the back-azimuth from the station; T_0, the period of the seismometer; T_g, the period of the galvanometer; Damp, the damping; Vm, the instrument amplification; Speed, the rotating drum velocity; Take-off, the angle for a seismic ray leaving the source.

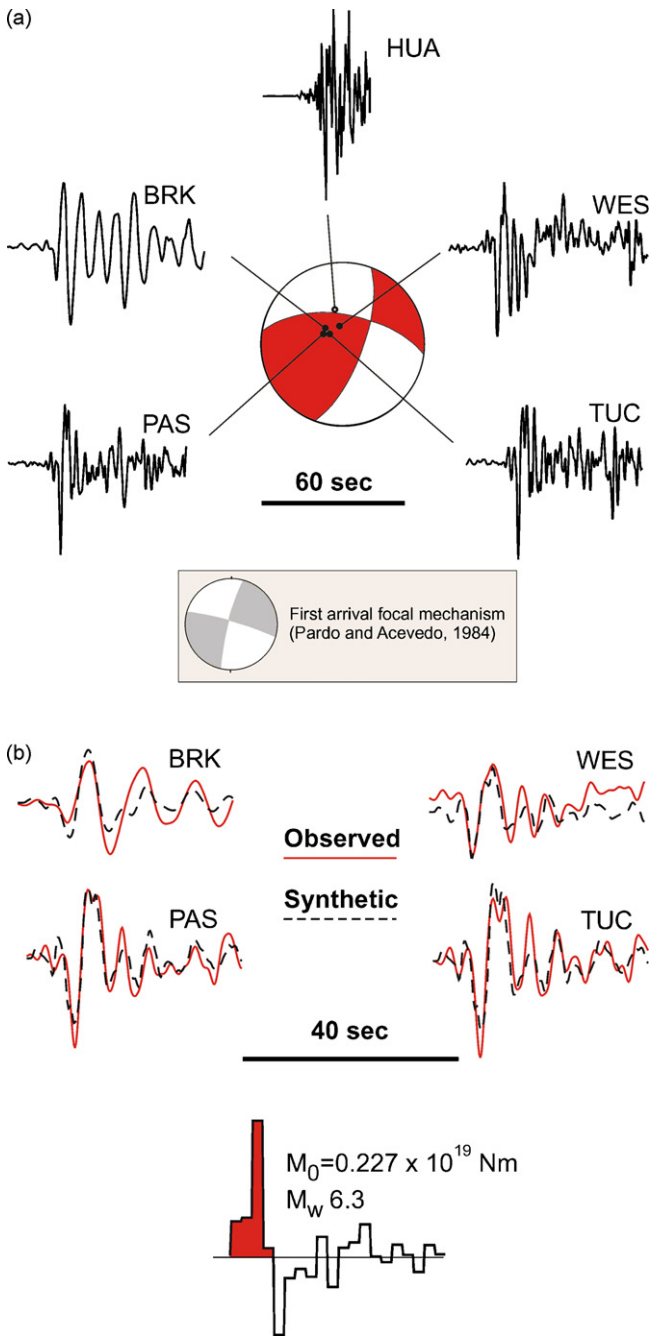

Fig. 8. Results of the 4 September 1958 Chile, earthquake. (a) Our preferred focal mechanism solution (fault plane_1: strike N20°E, dip 70° to the southeast and rake 30°; fault plane_2: strike N80°W, dip 62° to the north and rake 157°) plotted as a lower-hemisphere projection with dark compressional quadrants and P-wave seismic records (see Table 3 for details). For comparison, we present the first-motion focal mechanism solution from Pardo and Acevedo (1984). (b) Teleseismic modeling of the long period P-wave vertical component seismograms recorded at stations shown in Fig. 7b and Table 3; source time function results for the preferred focal mechanism. Solid lines are observed data and dashed lines are the synthetic data for our preferred model.

ing our seismic moment estimation ($M_0 = 0.227 \times 10^{19}$ N m) and the relationship $M_w = 0.67 \times \log M_0 - 6.0$, we obtained a moment magnitude $M_w = 6.3$. Our preferred focal mechanism solution indicates two possible fault planes: fault plane_1 with azimuth of 20°, dip of 70° to the southeast and rake of 30°; and fault plane_2 with azimuth of 280°, dip of 62° to the north and rake of 157°. Our best focal depth is about 8 km but solutions between 5 km and 9 km are acceptable. We obtained one single pulse for the source time

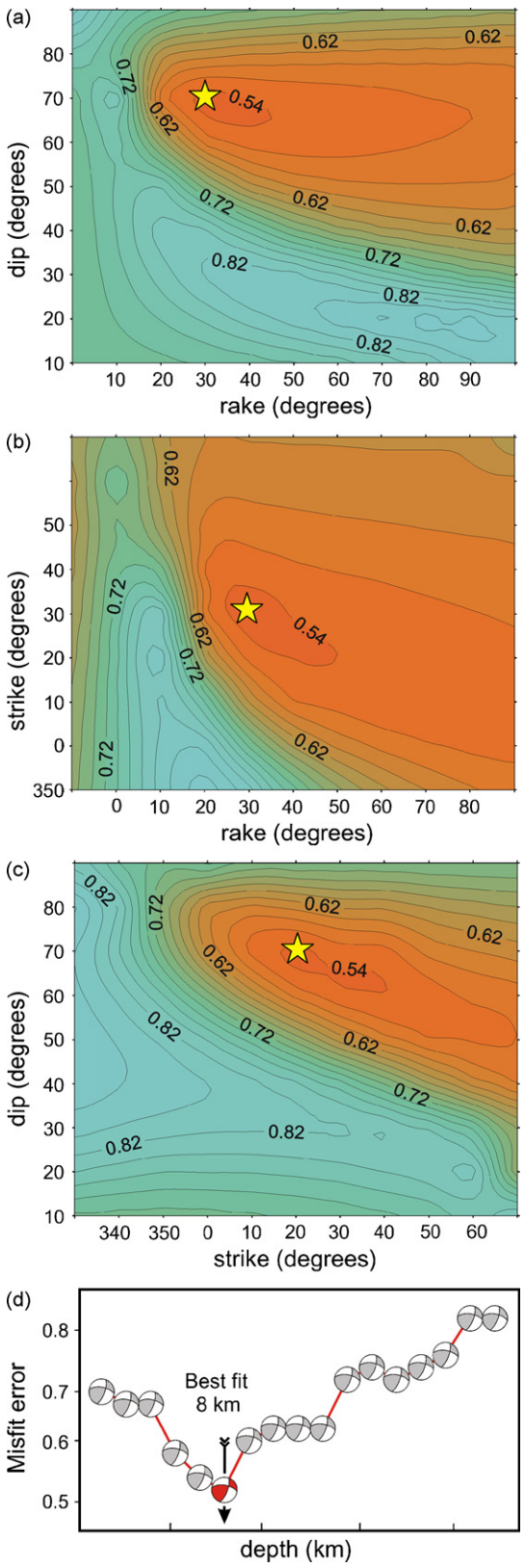

Fig. 9. Grid search results for focal mechanism parameters for the 1958 Las Melosas, Chile earthquake using multi-station inversion of long period P-wave seismograms. (a) Normalized errors between synthetic and observed seismogram-amplitudes for varying dip and rake for a fixed strike of N20°E. (b) Same as (a) varying strike and rake for a fixed dip of 70° to the southeast. (c) Same as (a) varying strike and dip for a fixed rake of 30°. (d) Synthetic and observed amplitude misfit errors as a function of focal depth for the best combination of strike, dip and rake (Fig. 8) and variable focal depth.

function of the first event (E1) during the sequence of the 1958 earthquake of a duration of 8–10 s (Fig. 8b), suggesting that most of the moment release occurred near the epicenter. Assuming a rupture velocity of 2.5 km s^{-1} and a duration of 8-s for the source time function, we estimate that most of the seismic moment was released within approximately 20 km of the epicenter. Depending on if the earthquake had a unilateral or bilateral rupture, the fault length should be between 20 km and 40 km, respectively. Using $M_0 = \mu DA$, and two possible fault areas (10 km × 20 km for a unilateral rupture and 10 km × 40 km for a bilateral rupture), and a rigidity μ of 3×10^{10} N m^{-2}, we calculated an average slip (D) of 40 cm and 20 cm, respectively.

In order to provide uncertainties, we have tested a full combination of source parameters (strike, dip, rake and focal depth) using a grid search. For this purpose we initially fixed the strike and varied the other parameters every ten degrees for the focal mechanism solution and every 1-km for the focal depth using the teleseismic P-wave inversion described in the previous section. We repeated the same analysis for a fixed dip, and then for a fixed strike. Different maps of the errors between the observed and synthetic data are shown in Fig. 9. Each point in these maps corresponds to a solution similar to that one shown in Fig. 8. Thus we constrained the overall best solution (Fig. 8) by comparing the observed seismograms (waveform and amplitude) to the synthetic seismograms calculated for a specific set of source parameters, the normalized errors between the synthetic and observed waveform amplitudes for each model, and the source time function results. We obtained possible ranges of 10–30° for the strike, 60–70° for the dip, and 20–40° for the rake (Fig. 9). We note these uncertainties in fault parameters are similar to those for the other east-west oriented fault plane solution. The best fit between observed and synthetic waveform amplitudes occur for a focal depth of 8 km, although solutions between 5 and 9-km depth are acceptable. Comparing our best solution for the 1958 earthquake to solutions for other moderate magnitude sized events in the region in 1987, 2001 and 2004 (see Fig. 2a), we note the NNW- SSE P-axis orientation is somewhat different. The other events show mainly EW to SW-NE P-axis orientations. Based on this observation and published GPS velocity vectors in our study area that exhibit from west to east a rough clockwise rotation and a significant magnitude decay through the Andean cordillera (Brooks et al., 2003; Vigny et al., in this issue), the crustal earthquakes in 1987, 2001 and 2004 could be accommodating deformation with small right-lateral motion along approximate north-south faults in the High Cordillera (Figs. 1b and 2a). In fact the 1987 M_w 5.9 crustal earthquake (Fig. 2a) and its aftershock sequence have occurred along an approximate north-south fault associated with right-lateral displacement (Barrientos and Eisenberg, 1988). In contrast, our solution for the 1958 Las Melosas earthquake shows a different strike-slip focal mechanism that could be related to east-west oriented faults that showed right lateral motion. We suggest the activation of east-west trending structures is important to accommodate differences in tectonic shortening from north to south. Higher tectonic shortening has been reported to the north of 33°S, a region mainly characterized by thin-skinned deformation (Allmendinger et al., 1990; Kley et al., 1999; Ramos et al., 2002) which extends into the Andean backarc, sometimes causing large magnitude damaging crustal earthquakes in the Argentinean Precordillera (Alvarado and Beck, 2006). South of 33°S the region is characterized by thick-skinned deformation (Ramos et al., 1996) mainly restricted to the active volcanic arc; this may be a consequence of the interaction of the High Andean Cordillera morphological unit with the rigid undeformed Argentinean basement in the backarc region where the Precordillera and Sierras Pampeanas uplifts exhibit their southern termination (Fig. 2) (Lavenu and Cembrano, 1999; Costa et al., 2000). In addition, for this region the ongoing upper plate deformation viewed from GPS measurements coincides with the signal of long-term geological deformation, also providing evidence of a progressive southward decrease of shortening velocity (Klotz et al., 2006). Nevertheless the occurrence of the 1958 Las Melosas earthquake along a north-south active fault cannot be ruled out.

Geomorphologic studies of the landslides triggered by the 1958 earthquakes show that the landslide in "Las Cortaderas" along the Yeso river (Fig. 2) was directly related to the event on 4 September of 1958 and the landslide in "El Manzanito" along the Maipo Valley south of Las Melosas was directly related to the event on 28 August of 1958 (see Sepúlveda et al., 2008 for a full description). Approximate 15–20 × 10^6 m^3 of mass consisting of volcanic blocks with sand were displaced during the 4 September event in a northwest direction along the approximately north-south oriented Yeso river (Flores et al., 1960; Casas et al., 2005). This is consistent with our focal mechanism solution associated with an active fault plane of north-south trending and the assumption that the Las Cortaderas landslide occurred along an active north-south fault during the 4 September 1958 earthquake. The possible active fault of north-south trending in our solution is also consistent with the dominant structural trend observed for the main morphostructural units and some Pliocene and Quaternary faults in the intra-arc Andean region (Lavenu and Cembrano, 1999; Armijo et al., 2006) (Figs. 1b and 2a). However, the left lateral motion predicted along a north-south active fault by our focal mechanism solution precludes the possible association of the 1958 earthquake to the recognized active faults in the Las Melosas epicentral area, which clearly show slips of tenths of kilometers in the last 20 m.a. along an east-west direction (Rolando Armijo, personal communication 2007; Lavenu and Cembrano, 1999).

According to Wells and Coppersmith (1994), an empirical scaling relationship between the moment magnitude and the surface rupture length (SRL) is given by $M_w = 5.08 + 1.16 \times \log$ (SRL). Using this relationship with our results, a surface rupture length of at least 11 km should be expected for the 1958 event, but no surface rupture caused by the 1958 earthquake has been reported. Thus the discrimination of the active fault plane in our focal mechanism solution and its association to exposed faults in the epicentral area are difficult (Pardo and Acevedo, 1984; Lavenu and Cembrano, 1999). More geomorphic features are needed to better delineate active structures in this area prone to landslides.

Refined focal-depth determinations from this study (8 km) and Alvarado et al. (2005), and crustal structure studies along the active arc (Alvarado et al., 2007) indicate the seismicity in the high Andes occurs in the upper crustal levels with focal depths < 20 km. This shows a different style of crustal deformation when compared with deeper (focal depths < 35 km) seismicity near Santiago to the west of the region of study (see Leyton et al., in this issue) or further east in Argentina (Alvarado et al., 2005).

Our estimations for the focal depth (~8 km) and focal mechanism (strike-slip solution) are consistent with previous seismic determinations by Lomnitz (1960), Piderit (1961) and Pardo and Acevedo (1984) (Fig. 8a). Both, constraints for the focal depth and focal mechanism are also in agreement with mechanical models by Armijo et al. (2006) that consider active major thrust structures at deeper levels in the western flank of the Principal Andean Cordillera (ex. San Ramón thrust fault).

Another interesting aspect of our study is related to the magnitude estimation. We find a moment magnitude M_w of 6.3; this is 0.4–0.7 units less than those previously reported by other authors (ex. Lomnitz, 1970a). We note the magnitude estimations M_s 6.75–7 (PAS); 6.75 (BRK) initially reported by the USCGS for event E1 on 4 September 1958 refer to an estimate of the Richter magnitude by the Seismological Laboratory at Pasadena (PAS, USA) or the Seismograph Station at Berkeley (BRK, USA) (BSSA, 1959). In contrast, our estimation of M_w 6.3 is based on source modeling directly related

to the radiated energy (Hanks and Kanamori, 1979) where seismogram amplitudes are taken into consideration but a higher weight is given to a good overall waveform fit than to a particular seismogram amplitude only. Other magnitudes reported (ex. M_s 6.9 by Lomnitz, 1970a) are based on seismic intensities which do not provide objective estimates of the uncertainty in magnitude in comparison with moment magnitude based on seismogram modeling. In fact good estimates of magnitudes using intensity data depend on intensity assignments which usually are few and more poorly determined for historical earthquakes (Bakun, 2006). It is worth to note that the seismic intensities reported for the 1958 earthquake can be reflecting the overall (integrated) effects of the three events E1, E2 and E3 on the seismic sequence of 4 September 1958, perhaps overestimating the magnitude of this earthquake. For these reasons we believe our estimation for M_w provides a more reliable estimate to quantify the 1958 Las Melosas seismic source.

A $M_w = 6.3$ event is associated with a rupture area of about 150–200 km^2 (or 20 km × 10 km), much less than the 800 km^2 expected for a 6.9 event (Wells and Coppersmith, 1994). We note, however, that our M_w estimation represents a lower limit because the best source time function results exhibit a slight negative pulse after the main positive pulse, which decreases the seismic moment estimation and thus our estimated magnitude. Adding more seismic records to the waveform modeling could improve these results.

The revised intensity data provide quantitative constraints on the attenuation of intensity as a function of distance. Compared with other crustal earthquakes, the intensity attenuation has similar patterns of shallow earthquakes in western Argentina and northern Chile, but damage caused by Las Melosas earthquake lies under the California earthquake attenuation relationships (Sepúlveda et al., 2008).

Our results and the two medium to large and well preserved landslides triggered by the 1958 earthquake in the epicentral area (Las Cortaderas and El Manzanito landslides) and the 1850 earthquake also associated with rockslides in the epicentral area of the 4 September 1958 earthquake (Fig. 2a) confirm that large landslides can occur for moderate crustal events and I_{MSK} or MMI ≥ VIII (Boatwright and Bundock, 2005). Based on historic information no site amplifications derived from superficial geology deposits were detected for the damage area (Table 2).

7. Conclusions

Inversion of teleseismic P-waves for the first event in the sequence of earthquakes on 4 September 1958 indicates a strike-slip focal mechanism solution with fault planes of: (1) azimuth = 20°, dip 70° to the southeast and rake 30° and (2) azimuth = 280°, dip = 62° to the northeast and rake = 157°, a focal depth of 8 km, a seismic moment M_0 of 0.227×10^{19} N m and a moment magnitude M_w of 6.3. We found a simple source time function of 8–10 s duration.

This strike-slip solution for the crustal 1958 M_w 6.3 earthquake with NNW-SSE P-axis orientation indicates a discordant style of earthquake deformation when compared to other strike-slip solutions in the region for moderate earthquakes in 1987, 2001 and 2004 that show mainly east-west P-axis orientations and agreement with E-W compression patterns in the High Cordillera since Pliocene. Although no surface rupture was reported for the 1958 Las Melosas event, our solution for this earthquake is more consistent with the activation of east-west structures, which could be accommodating differences in a higher shortening to the north of ~33°S than to the south of this latitude.

Large-sized crustal seismicity in the High Andean Cordillera between 30°S and 35°S seems to be rare during historical and present times (Gustcher et al., 2000). The occurrence of the crustal earthquake on 4 September 1958 indicates the potential for damaging moderate magnitude strike-slip events associated to undetected active faults that can seismically trigger landslides and rockslides in a populated area to the east of Santiago. Thus, the intensity results provide important information on the level of shaking that can be expected from shallow crustal earthquakes in central Chile, and should be considered in seismic hazard assessments and engineering design in the region. Considering the maximum expected intensities for a shallow design earthquake (M ~7.0, I_{MSK} ~IX), the Chilean seismic code must prohibit the construction of adobe and unreinforced masonry buildings.

Acknowledgements

The authors would like to acknowledge the NSF grant EAR-0510966, the National PERISHIP Dissertation Award (2004), PICT2006-0122 and UNSJ-CICITCA 21/E814 and the Millenium Nucleous of Seismotectonics and Seismic Hazards. We thank Victor Ramos and an anonymous reviewer for their reviews and suggestions that helped to improve this paper. We thank Rolando Armijo for fruitful discussions. Maps were generated using Generic Mapping Tools (Wessel and Smith, 1991).

References

Allmendinger, R.W., Figueroa, D., Snyder, D., Beer, J., Mpodozis, C., Isacks, B.L., 1990. Foreland shortening and crustal balancing in the Andes at 30°S latitude. Tectonics 9 (4), 789–809.

Alvarado, P.M., 1998. Sismicidad superficial de los Andes Centrales (33°–35°S; 69.5°–70.5°W). M.Sc. Thesis. Facultad de Ciencias Físicas y Matemáticas, Universidad de Chile, Chile, p. 161 (in Spanish).

Alvarado, P., Beck, S., 2006. Source characterization of the San Juan (Argentina) Crustal Earthquakes of 15 January 1944 (M_w 7.0) and 11 June 1952 (M_w 6.8). Earth Planet. Sci. Lett. 243 (3–4), 615–631, doi:10.1016/j.epsl.2006.01.015.

Alvarado, P., Beck, S., Zandt, G., Araujo, M., Triep, E., 2005. Crustal deformation in the south-central Andes back-arc terranes as viewed from regional broadband seismic waveform modelling. Geophys. J. Int. 163 (2), 580–598, doi:10.1111/j.1365-246X.2005.02759.x.

Alvarado, P., Beck, S., Zandt, G., 2007. Crustal structure of the south-central Andes Cordillera and backarc region from regional waveform modelling. Geophys. J. Int. 170 (2), 858–875, doi:10.1111/j.1365-246X.2007.03452.x.

Alvarado, P., Pardo, M., Gilbert, H., Miranda, S., Anderson, M., Saez, M., Beck, S., 2009. Flat-slab subduction and crustal models for the seismically active Sierras Pampeanas region of Argentina. In: Kay, S.M., Ramos, V.A., Dickinson, W.R., (Eds.), Backbone of the Americas: Shallow subduction, plateau uplift, and ridge and terrane collision. Geological Society of America Memoir 204, Chapter 12, doi:10.1130/2009.1204(12).

Anderson, M., Alvarado, P., Beck, S., Zandt, G., 2007. Geometry and brittle deformation of the subducting Nazca plate, Central Chile and Argentina. Geophys. J. Int. 171 (1), 419–434.

Armijo, R., Rauld, R., Thiele, R., Vargas, G., Campos, J., Lacassin, R., Kausel, E., 2006. Tectonics of the western front of the Andes and its relation with subduction processes: The San Ramón Fault and associated seismic hazard for Santiago (Chile). Montessus Abstract N (ST1-03), Chile, 2006. http://www.dgf.uchile.cl/montessus/abstract/Armijo.htm.

Astroza, M., Sepúlveda, S., 2006. Intensity and ground shaking estimates of the September 1958 Las Melosas earthquake. Montessus Abstract N (GT3-01), Chile, 2006.

Bakun, W.H., 2006. Estimating locations and magnitudes of earthquakes in Southern California from Modified Mercalli intensities. Bull. Seismol. Soc. Am. 96 (4A), 1278–1295, doi:10.1785/0120050205.

Baldis, B., Bordonaro, O., 1981. Evolución de las facies carbonáticas en la cuenca Cámbrica de la Precordillera de San Juan, VIII Argentinean Geological Congress 2, San Luis, Argentina, pp. 385–397.

Barazangi, M., Isacks, B.L., 1976. Spatial distribution of earthquakes and subduction of the Nazca Plate beneath South America. Geology 4, 686–692.

Barrientos, S., 2007, Earthquakes in Chile. In: Moreno, T., Gibbons, W. (Eds.), The Geology of Chile, 424 pp., Geological Society, London, United Kingdom, 263–287. ISBN 978-1-86239-220-5.

Barrientos, S., Eisenberg, A., 1988. Secuencia sísmica en la zona cordillerana al interior de Rancagua. V Congreso Geológico Chileno, Santiago, Chile, pF121–F132.

Barrientos, S., Vera, E., Alvarado, P., Monfret, T., 2004. Crustal seismicity in Central Chile. J. South Am. Earth Sci. 16, 759–768.

Barrientos, S., Ward, S., 1990. The 1960 Chile earthquake—inversion for slip distribution from surface deformation. Geophys. J. Int. 103, 589–598.

Beck, S., Barrientos, S., Kausel, E., Reyes, M., 1998. Source characteristics of historic earthquakes along the central Chile subduction zone. J. South Am. Earth Sci. 11, 115–129.

Boatwright, J., Bundock, H., 2005. Modified Mercalli Intensity Maps for the 1906 San Francisco Earthquake plotted in ShakeMap Format, U.S. Geol. Surv. Open-File Report, 1135.
Bromirski, P.D., Chuang, S., 2003. SeisDig: Software to digitize scanned analog seismogram images. University of San Diego, USA, p. 28.
Brooks, B.A., Bevis, M., Smalley R.Jr., Kendrick, E., Manceda, R., Lauría, E., Maturana, R., Araujo, M., 2003. Crustal motion in the southern Andes (26°–36°S): do the Andes behave like a microplate? Geochem. Geophys. Geosyst. 4 (10), 1–14, doi:10.1029/2003GC000505.
BSSA, 1959. Seismological notes. Bull. Seismol. Soc. Am. 49(1) 115–118.
Cahill, T., Isacks, B., 1992. Seismicity and shape of the subducted Nazca plate. J. Geophys. Res. 97, 17503–17529.
Casas, E.A., Sepúlveda, S.A., Campos, J., Rebolledo, S., 2005. Estudio del terremoto de Las Melosas de 1958 mediante caracterización de deslizamientos cosísmicos, IX Jornadas Chilenas de Sismología e Ingeniería Antisísmica, Article A01-06, 8 pp., 16–19 de Noviembre de 2005, Concepción–Chile.
Charrier, R., Baeza, O., Elgueta, S., Flynn, J., Gans, P., Kay, S., Muñoz, N., Wyss, A., Zurita, E., 2002. Evidence for Cenozoic extensional basin development and tectonic inversion south of the flat-slab segment southern Central Andes, Chile (33°–36° S.L.). J. South Am. Earth Sci. 15, 117–139.
Charrier, R., Farías, M., Comte, D., Pardo, M., 2004. Active tectonic in the Southern Central Andes, a recent example: the 28 August, 2004 shallow M_w = 6.5 earthquake, Eos Trans. American Geophysical Union, 85(47), Fall meeting abstracts, Abstract S43C-1015, San Francisco, U.S.A.
Charrier, R., Pinto, L., Rodriguez, M.P., 2007. Tectonostratigraphic evolution of the Andean Orogen in Chile. In: Moreno, T., Gibbons, W. (Eds.), The Geology of Chile, 424 pp. Geological Society, London, United Kingdom, pp. 21–114. ISBN 978-1-86239-220-5.
Cifuentes, I., 1989. The 1960 Chilean earthquakes. J. Geophys. Res. 94, 665–680.
Cisternas, M., Atwater, B.T., Torrejón, F., Sawai, Y., Machuca, G., Lagos, M., Eipert, A., Youlton, C., Salgado, I., Kamataki, T., Shishikura, M., Rajendran, C.P., Malik, J.K., Rizal, Y., Husni, M., 2005. Predecessors of the giant 1960 Chile earthquake. Nature 437, 404–407, doi:10.1038/nature03943.
Costa, C.H., Gardini, C.E., Diederix, H., Cortés, J.M., 2000. The Andean orogenic front at Sierra de Las Peñas-Las Higueras, Mendoza, Argentina. J. South Am. Earth Sci. 13 (3), 287–292, doi:10.1016/S0895-9811(00)00010-9.
Cristallini, E., Ramos, V., 2000. Thick-skinned and thin-skinned thrusting in the La Ramada fold and thrust belt: crustal evolution of the High Andes of San Juan, Argentina (32°SL). Tectonophysics 317, 205–235.
DIC, 1958. Archivo fotográfico, División Estructura-Construcción-Geotecnia, Departamento de Ingeniería Civil, Facultad de Ciencias Físicas y Matemáticas, Universidad de Chile, Santiago, Chile.
El Correo de Santiago, 2009. Terremoto 04 septiembre 1958 Las Melosas, http://mundo21.tripod.com/17h1958lasmelosas.html.
El Mercurio de Santiago, 1958. Santiago, Chile, Edition of 5th of September, 1958.
Engdahl, E.R., van der Hilst, R.D., Buland, R., 1998. Global teleseismic earthquake relocation with improved travel times and procedures. Bull. Seism. Soc. Am. 88, 722–743.
Flores, R., Arias, S., Jenshke, V., Rosenberg, L.A., 1960. Engineering aspect of the earthquakes in the Maipo Valley, Chile, in 1958. In: Proceedings of 2nd World Conference in Earthquake Engineering, vol. 1. Japan, pp. 409–431.
Giambiagi, L.B., Ramos, V.A., 2002. Structural evolution of the Andes in a transitional zone between flat and normal subduction (33°30′–33°45′S), Argentina and Chile. J. South Am. Earth Sci. 15 (1), 101–116.
Giambiagi, L., Alvarez, P., Godoy, E., Ramos, V.A., 2003. The control of pre-existing extensional structures on the evolution of the southern sector of the Aconcagua fold and thrust belt, southern Andes. Tectonophysics 369, 1–19.
Goldstein, P., Dodge, D., Firpo, M., 1999. SAC2000: signal processing and analysis tools for seismologists and engineers, UCRL-JC-135963. Invited Contribution to the IASPEI International Handbook of Earthquake and Engineering Seismology.
Gustcher, M., Spakman, W., Bijwaard, H., Engdahl, R., 2000. Geodynamics of flat subduction: seismicity and tomographic constraints from the Andean margin. Tectonics 19, 814–833.
Hanks, T.C., Kanamori, H., 1979. A moment magnitude scale. J. Geophys. Res. 84 (B5), 2348–2350.
Harvard Centroid Moment Tensor database, 2009. on-line catalogue www.globalcmt.org.
Hoffmann-Rothe, A., Kukowski, N., Dresen, G., Echtler, H., Oncken, O., Klotz, J., Scheuber, E., Kellner, A., 2006. Oblique convergence along the Chilean margin: partitioning, margin-parallel faulting and force interaction at the plate interface. In: Oncken, O., Chong, G., Franz, G., Giese, P., Götze, H-J., Ramos, V.A., Strecker, M.R., Wigger, P. (Eds.), The Andes–active subduction orogeny. *Frontiers in Earth Science Series*, Part II, Chapter 6, vol. 1. Springer-Verlag, Berlin, Heidelberg, New York, pp. 125–146, 507 pp. ISBN: 978-3-540-24329-8, doi:10.1007/978-3-540-48684-8_6.
INPRES, 2009. Listado de terremotos históricos de Argentina. On-line catalogue www.inpres.gov.ar.
Jordan, T.E., Allmendinger, R.W., 1986. The Sierras Pampeanas of Argentina: a modern analogue of Rocky Mountain foreland deformation. Am. J. Sci. 286, 737–764.
Jordan, T.E., Isacks, B.L., Allmendinger, R.W., Brewer, J.A., Ramos, V.A., Ando, J.C., 1983. Andean tectonics related to geometry of subducted Nazca plate. Geol. Soc. Am. Bull. 94, 341–361.
Kadinsky-Cade, K., 1985. Seismotectonic of the Chilean margin and the 1977 Caucete earthquake of western Argentina. PhD Thesis. Cornell University, Ithaca, New York, U.S.A., p. 253 (in English).
Karnik, V., Schenkova, Z., Schenk, V., 1984. Vulnerability and the MSK Scale. Eng. Geol. 20, 161–168.
Kausel, E., 1991. The influence of large thrust and normal earthquakes in the assessment of the seismic hazard, Workshop: New Horizons in Strong Ground Motion: Seismic Studies and Engineering Practice, Santiago, Chile.
Kausel, E., Campos, J., 1992. The M = 8.0 tensional earthquake of December 9, 1950 of northern Chile and its relation to the seismic potential of the region. Phys. Earth Planet. Interiors 72, 220–235.
Kay, S.M., Mpodozis, C., Ramos, V.A., Munizaga, F., 1991. Magma source variations for mid-late Tertiary magmatic rocks associated with a shallowing subduction zone and a thickening crust in the central Andes (28° to 33°S) Argentina. In: Harmon, R.S., Rapela, C.W. (Eds.), Andean Magmatism and Its Tectonic Setting. Boulder, Colorado, U.S.A., Geological Society of America Special Paper 265, pp. 113–137.
Kley, J., Monaldi, C.R., Salfity, J.A., 1999. Along-strike segmentation of the Andean foreland: causes and consequences. Tectonophysics 301, 75–94.
Klotz, J., Abolghasem, A., Khazaradze, G., Heinze, B., Vietor, T., Hackney, R., Bataille, K., Maturana, R., Viramonte, J., Perdomo, R., 2006. Long-term signals in the present-day deformation field of the Central and Southern Andes and constraints on the viscosity of the Earth's upper mantle. In: Oncken, O., Chong, G., Franz, G., Giese, P., Götze, H-J., Ramos, V.A., Strecker, M.R., Wigger, P. (Eds), The Andes–active Subduction Orogeny. *Frontiers in Earth Science Series*, Part I, Chapter 4, vol. 1. Springer-Verlag, Berlin, Heidelberg, New York, pp. 65–89, 570 pp. ISBN: 978-3-540-24329-8, doi:10.1007/978-3-540-48684-8_4.
Langer, C.J., Hartzell, S., 1996. Rupture distribution of the 1977 western Argentina earthquake. Phys. Earth Planet. Interiors 94, 121–132.
Lavenu, A., Cembrano, J., 1999. Compressional- and transpressional-stress pattern for Pliocene and Quaternary brittle deformation in fore arc and intra-arc zones (Andes of Central and Southern Chile). J. Struct. Geol. 21 (12), 1669–1691, doi:10.1016/S0191-8141(99)00111-X.
Leyton, F., Perez, A., Campos, J., Rauld, R., Kausel, E., 2009. Anomalous seismicity in the lower crust of the Santiago Basin, Chile. Phys. Earth Planet. Interiors 175, 17–25.
Lomnitz, C., 1960. A study of the Maipo Valley earthquakes of September 4, 1958. In: Proc. 2nd World Conf. Earthq. Eng., 1. Tokyo-Kyoto, Japan, pp. 501–520.
Lomnitz, C., 1970a. Casualties and behavior of populations during earthquakes. Bull. Seism. Soc. Am. 60 (4), 1309–1313.
Lomnitz, C., 1970b. Major earthquakes and Tsunamis in Chile during the period 1535 to 1955. Geologische Rundschau 59 (3), 938–960.
Mingorance, F., 2006. Morfometría de la escarpa de falla histórica identificada al norte del cerro La Cal, zona de falla La Cal, Mendoza. Revista de la Asociación Geológica Argentina 61 (4), 620–638, ISSN 0004-4822.
Monge, J. Astroza, M., 1989. Metodología para determinar el grado de intensidad a partir de los daños, Actas V[as] Jornadas Chilenas de Sismología e Ingeniería Antisísmica, Vol. 1, Santiago, Chile, pp. 483–491.
Parada, M., Levi, B., Nystrom, J.O., 1991. Geochemistry of the Triassic to Jurassic plutonism of Central Chile (30 to 33°S); petrogenetic implications and a tectonic discussion. In: Harmon, R.S., Rapela, C.W. (Eds.), Andean magmatism and its tectonic setting (special issue). Geol. Soc. Am. Special Paper 265, pp. 99–112.
Pardo, M., Comte, D., Monfret, T., Boroschev, R., Astroza, M., 2002. The October 15, 1997 Punitaqui earthquake (Mw = 7.1): a destructive event within the subducting Nazca plate in central Chile. Tectonophysics 345 (1–4), 199–210, doi: 10.1016/S0040-1951(01)00213-X.
Pardo, M., Acevedo, P., 1984. Mecanismos de foco en la zona de Chile Central. Tralka 2 (3), 279–293.
Peyrat, S., Campos, J., Chabalier, J.B., de Perez, A., Bonvalot, S., Bouin, M.-P., Legrand, D., Nercessian, A., Charade, O., Patau, G., Clévédé, E., Kausel, E., Bernard, P., Villote, J.-P., 2006. Tarapacá intermediate-depth earthquake (Mw 7.7, 2005, northern Chile): A slab-pull event with horizontal fault plane constrained from seismologic and geodetic observations. Geophys. Res. Lett. 33, L22308, doi:10.1029/2006GL027710.
Piderit, E., 1961. Estudios de los sismos del Cajón del Maipo en el año 1958. In: Memoria para optar al Título de Ingeniero Civil. Facultad de Ciencias Físicas y Matemáticas, Universidad de Chile, Santiago, Chile.
Ramos, V.A., 1999, Las provincias geológicas del territorio Argentino. In: Caminos, R. (Ed.), Geología Argentina, Caminos, 804 pp. Anales 29(3), 41–96. *Dirección Nacional del Servicio Geológico*, Buenos Aires, Argentina.
Ramos, V.A., Cegarra, M., Cristallini, E.O., 1996. Cenozoic tectonics of the high Andes of west-central Argentina (30-36 degrees S latitude) (in Geodynamics of the Andes). Tectonophysics 259 (1–3), 185–200.
Ramos, V.A., Cristallini, E.O., Perez, D.J., 2002. The Pampean flat-slab of the Central Andes. J. South Am. Earth Sci. 15 (1), 59–78.
Rosenberg, L.A., 1958, Informe visita a la zona dañada por los terremotos del Cajón del Maipo, Unpublished Report, Civil Engineering Department, University of Chile, Santiago, Chile.
Ruff, L., 1989. Multi-trace deconvolution with unknown trace scale factors: omnilinear inversion of P and S waves for source time functions. Geophys. Res. Lett. 16, 1043–1046.
Saint-Amand, P., Ericksen, G.E., 1964. Las Melosas-El Volcán, Chile, earthquake swarm of August and September 1958, Geol. Soc. Am. Special Paper 76, pp. 222–223.
Sepúlveda, S., Astroza, M., Kausel, E., Campos, J., Casas, E., Rebolledo, S., Verdugo, R., 2008. New findings on the 1958 Las Melosas earthquake sequence, Central Chile: implications for seismic hazard related to shallow crustal earthquake in subduction zones. J. Earthquake Eng. 12, 432–455, doi:10.1080/13632460701512951.
Stern, C.R., 2004. Active Andean volcanism: its geologic and tectonic setting. Rev. Geol. Chile 31 (2), 161–206.

Thiele, R., 1980. Hoja Santiago, Instituto de Investigaciones Geológicas. Carta Geológica de Chile 39, 21.
Tichelaar, B.W., Ruff, L.J., 1991. Seismic coupling along the Chilean subduction zone. J. Geophys. Res. 96 (B7), 11997–12022.
Vietor, T., Echtler, H., 2006. Episodic Neogene southward growth of the Andean subduction orogen between 30°S and 40°S–plate motions, mantle flow, climate, and upper-plate structure. In: Oncken, O., Chong, G., Franz, G., Giese, P., Götze, H-J., Ramos, V.A., Strecker, M.R., Wigger, P. (Eds.), The Andes–active subduction orogeny. *Frontiers in Earth Science Series*, Part III, Chapter 18, vol. 1. Springer-Verlag, Berlin, Heidelberg, New York. pp. 375–400, 507 pp. ISBN: 978-3-540-24329-8, doi:10.1007/978-3-540-48684-8_18.
Vigny, C., Rudloff, A., Ruegg, J.C., Madariaga, R., Campos, J., Alvarez, M., 2009. Upper plate deformation measured by GPS in the Coquimbo Gap Chile. Phys. Earth Planet. Interiors 175, 86–95.
Wells, D., Coppersmith, K., 1994. New empirical relationships among magnitude, rupture length, rupture width, rupture area and surface displacement. Bull. Seism. Soc. Am. 84, 974–1002.
Wessel, P., Smith, W.H.F., 1991. Free software helps map and display data. Eos Trans. Am. Geophys. Un. 72, 445–446, p. 441.
Yañez, G., Ranero, C.R., von Huene, R., Diaz, J., 2001. Magnetic anomaly interpretation across the southern central Andes (32°–34°S): The role of the Juan Fernández Ridge in the late Tertiary evolution of the margin. J. Geophys. Res. 106 (B4), 6325–6345.
Zamarbide, J.L., Castano, J.C., 1993. Analysis of the January 26th, 1985, Mendoza (Argentina) earthquake effects and of their possible correlation with the recorded accelerograms and soil conditions. Tectonophysics 218, 221–235.